OPEN ACCESS

International
Journal
Of Modern Engineering Research (IJMER)

Numerical Investigation of Ice Accumulation and Accretion over an Airfoil Using FENSAP-ICE Solver

[a]Swetha S, [b]AbdulSharief, [c]S. K. Maharana

[a]*Asst Professor Dept. of Aeronautical Engineering, Acharya Institute of Technology, Bangalore-560107*
[b]*Professor, Dept. of Mechanical Engineering, P.A. College of Engineering, Mangalore-574153*
[c]*Professor, Dept. of Aeronautical Engineering, Acharya Institute of Technology, Bangalore-560107*
Corresponding Author: Swetha S

ABSTRACT: *Since the beginning of civil aviation, icing is a severe weather hazard for aircraft operation.For many years, the term engine icing has been used to describe ice accreting on exposed engine surfaces as an aircraft flies through a cloud of super-cooled liquid droplets. Since the beginning of aeronautical engineering, aircraft icing has been a great issue to flight safety. Consequently, research on this topic is ongoing for decades. The accreting ice variously affects the aerodynamic characteristics and controllability of the aircraft depending on the location of ice accretions and their amount and type. In the most general case, the icing of the airfoils of an aircraft can lead to a decrease in its lift force and angle of stall on the wing and on the tail assembly elements and to cause the loss of longitudinal stability of the apparatus. It has been a complex physical situation to comprehend the accretion process and its impact. In the present study a NACA0012 airfoil geometry has been used to understand the accumulation and accretion process through simulation. Ansys® FENSAP-ICE solver has been the platform wherein three different solvers such as FENSAP, DROP3D and ICE3D are used to compute the mass of ice accreted. The characteristic length of the airfoil is 0.914 m and Reynolds number of the flow is 7.4 x $10^6$and Mach number is 0.3. The results of total mass of ice accreted with respect to total time of accretion (t_{ice}) have been presented. The validation and verification of the simulation results has been done with the experimental data published by the past researchers.*

KEY WORDS: *Ice Accretion, Airfoil, RANS, Turbulent Flows, Droplet, Crystal, Viscous Flow*

Date of Submission: 16-01-2019 Date of acceptance: 28-01-2019

I. INTRODUCTION

Accretions of ice in the form of ridges or individual streaks, which are commonly called "barrier" ice, appear behind the protected zone on the aircraft surface. Since the occurring accidents with aircraft in the presence of large overcooled droplets in the atmosphere take place even if these apparatuses are equipped with an active anti-icing system, understanding the mechanism underlying the influence of the "barrier" ice on the aerodynamic characteristics and controllability of an aircraft is extremely important for ensuring the safety of its flight. It is necessary to understand the physics of ice accretion before describing further on the reason and the motivation to work further on this crucial topic. At flight altitude, high concentrations of particular small ice crystals are found which can rarely be detected by current on-board radar technology. Ice crystal concentrations are quantified by the ice water content (IWC)similar to the liquid water content (LWC) of super-cooled droplet clouds. The liquid water content is defined as the ratio of cumulative liquid droplet mass to the surrounding volume of air. At atmospheric temperatures above -40^{o}C, mixed phase clouds consisting of solid ice particles and liquid droplets can appear.

The water drops formed during snow thawing at a high altitude may pass through the zone with a temperature below zero (in the presence of temperature inversion) and become overcooled. In the past two decades, in connection with the rapid development of computer technologies, significant advances have been made in the field of modeling the aero hydrodynamic processes by solving two-dimensional Reynolds-averaged Navier–Stokes equations (RANS). To study the processes of the icing of aircraft wings and of the influence of "barrier" ice accretions on their aerodynamic characteristics, a number of investigations were carried out.

Thus, in Ref [1] the program code ARC2D, based on structured grids, was used to study the influence of ice accretions on the NACA0012 airfoil on its aerodynamic characteristics with the use of the Navier–Stokes equations for a thin layer together with the Baldwin–Lomax algebraic two-layer model of turbulence [2], and a comparison of the obtained results with experimental data was made. The results of calculations of the aerodynamic characteristics of the airfoil showed good agreement with the corresponding experimental data for angles of attack smaller than the angle of flow stall from the wing. Good agreement was also observed between the calculated and experimental data on pressure distribution over the surface of the airfoil except for the region of ice accretion. The averaged values of pressure on the airfoil surface were compared with a steady-state solution and experimental results. The model has been improved, but substantial deviations from experimental data were still observed.

In Ref [3-4], calculations were carried out with the use of RANS on rearrangable unstructured high-resolution grids located along the ice accretion surface on the leading edge of an airfoil. The data obtained were in good agreement with the results of corresponding calculations on unstructured grids. No comparison with experiments was made. It was established that the shape of the ice accretion on the airfoil surface can be determined as a function of time with account for the influence exerted by the outer air flow. The results of calculations of the forms of ice on an airfoil with the use of adaptive grids in solving the Navier–Stokes equations are presented in Ref [5]. The discretization of the initial equations was done by means of the Galerkin finite-volume method with application of the k–ε model of turbulence with wall functions. A number of shapes of ice accretions on the NACA0012 airfoil were considered, including ice "horns" on the loading edge, accretion in the form of a quadrant on the upper surface, and fine-scale roughness. Calculations were carried out for the Reynolds and Mach numbers Re = $3.1x10^6$ and Mach(M)= 0.15. The air flow field relative to this airfoil and the aerodynamic characteristics of the latter were obtained; however, no comparison was made with experimental data. The results of calculations revealed a considerable loss in the wing lift force because of the comb-shaped accretion of ice on the wing′s upper surface. It was much larger than the ice formation on the leading edge of the wing. In 1999 the results of comprehensive experimental investigations of the lift force, drag, and aerodynamic moment of the wing, as well as pressure distribution over its surface as a function of the shape of ice formations on the upper surface and leading edge of the wing, were published in Ref [6–8], which made it possible to compare the results of calculations with experimental data. A detailed comparison of the results of calculations obtained on unstructured grids with the use of full Navier–Stokes equations and of the NSU2D program code for a two-dimensional model of a NACA 23012 airfoil with ice accretion in the form of a quadrant on its upper surface was made in Ref [9]. The results of calculations showed good agreement with the corresponding experimental data up to the moment of flow stalling from the wing and an adequate effect of the size and location of ice accretions on the aerodynamic characteristics of the wing. Such investigations were later carried out [10] for other NACA airfoils in implementing the Glenn Research Center Program.

The objective of the proposed research is to understand and address these issues of ice accretion using a multiphase approach for an airfoil, which is one of the deciding geometric attributes for a fan blade design of a jet-based engine. The geometry considered is a NACA0012 airfoil.

II. GOVERNING EQUATIONS

Below are given the fundamental equations that are used during the study. These equations are used for the computations of the flow variables using ANSYS FANSAP-ICE solver.

Continuity equation:

$$\frac{\partial \rho_a}{\partial t} + \vec{\nabla}.\left(\rho_a V_a\right) = 0 \qquad (1)$$

Where, ρ is the density and V is the velocity vector. The subscript a refers to the air solution. This equation is also known as the continuity equation.

Momentum equation:

For a Newtonian fluid, Newton second law of motion states that the total force acting on a fluid particle is equal to the time rate of change of its momentum. This can be written in 3D using a set of 3 non-linear equations, shown here in vector form:

$$\frac{\partial \rho_a V_a}{\partial t} + \vec{\nabla}.\left(\rho_a \vec{V}_a \vec{V}_a\right) = \vec{\nabla}.\sigma^{ij} + \rho_a \vec{g} \qquad (2)$$

Where σ^{ij} is the stress tensor

$$\sigma^{ij} = -\delta^{ij} p_a + \mu_a \left[\delta^{jk}\nabla_k \upsilon^i + \delta^{ik}\nabla_k \upsilon^j - \frac{2}{3}\delta^{ij}\nabla_k \upsilon^k\right] = -\delta^{ij} p_a + \tau^{ij}$$

$$\tau^{ij} = \mu_a \left[\delta^{jk}\nabla_k \upsilon^i + \delta^{ik}\nabla_k \upsilon^j - \frac{2}{3}\delta^{ij}\nabla_k \upsilon^k\right]$$

p is the static pressure and μ is the dynamic viscosity. The special case of inviscid fluid flows, where the dynamic viscosity is set to zero, yields the Euler equations. For a viscous laminar flow, the viscosity is defined empirically by Sutherland law:

$$\frac{\mu_a}{\mu_\infty} = \left(\frac{T}{T_\infty}\right)^{3/2} \left(\frac{T_\infty + 110}{T + 110}\right)$$

Where, T refers to the static air temperature in Kelvin, and where the subscript ∞ indicates reference values for air: T_∞ = 288 K and $\mu\infty = 17.9 X10^{-6}$ Pa s.

Energy equation

The third physical principle concerns the conservation of energy and states that the total energy of the system must be conserved, or:

$$\frac{\partial \rho_a E_a}{\partial t} + \vec{\nabla}.\left(\rho_a \vec{V}_a \vec{H}_a\right) = \vec{\nabla}.\left(\kappa_a\left(\vec{\nabla}T_a\right) + \upsilon_i \tau^{ij}\right) + \rho_a \vec{g}.\vec{V}_a \qquad (3)$$

Where E and H are the total internal energy and enthalpy, respectively and κ is the thermal conductivity, computed in a similar way to the laminar dynamic viscosity:

$$\kappa = C1 * (T^{\frac{3}{2}})/(T + 133.7)$$

Where T refers to the static air temperature in Kelvin, and where the C1 is equal to 0.00216176W/(mK$^{3/2}$)

III. APPROACH

The approach will be both numerical and experimental to substantiate the outcome of the research. The very first approach is to numerically study the ice accumulation and accretion on an airfoil. The 3D partial differential equation-based equilibrium model introduced is derived based on the Messinger model. It has been further improved to predict the ice accretion and water runback on the surface [6]. The velocity $\mathbf{u}_f$ of the water in the film is a function of coordinates $\mathbf{x} = (x_1, x_2)$ on the surface and y normal to the surface. A simplifying assumption consists of taking a linear profile for $\mathbf{u}_f(\mathbf{x}, y)$, with a zero velocity imposed at the wall, i.e.:

$$\mathbf{u}_f(\mathbf{x}, y) = \frac{y}{\mu_w} \tau_{wall}(\mathbf{x}) \qquad (4)$$

where τ_{wall}, the shear stress from the air, is the main driving force for the water film.

By averaging across the thickness of the film, a mean water film velocity is obtained:

$$\bar{\mathbf{u}}_f(\mathbf{x}) = \frac{1}{h_f} \int_0^{h_f} \mathbf{u}_f(\mathbf{x}, y) dy = \frac{h_f}{2\mu_w} \tau_{wall}(\mathbf{x}) \qquad (5)$$

The resulting system of partial differential equations is thus the following mass conservation and energy conservation equations:

$$\rho_w \left[\frac{\partial h_f}{\partial t} + div\left(\overline{\mathbf{u}_f} h_f\right)\right] = U_\infty LWC\ \beta - \dot{m}''_{evap} - \dot{m}''_{ice} \qquad (6)$$

Where the three terms on the right-hand-side correspond to the mass transfer by water droplet impingement (source for the film), the evaporation and the ice accretion (sinks for the film), respectively.

IV. RESULTS AND DISCUSSION

Three numerical tools were used to simulate the ice accretion over an airfoil and a circular cylinder. The three modules are FENSAP-ICE, DROP3D and ICE3D. These are state-of-art icing code capable of 2D and 3D icing simulation for a large variety of applications. The flow field is simulated using a RANS [Reynold-Averaged- Navier-Stokes] flow solver, droplet and ice crystal impingement is simulated using an Eulerian approach; ice growth is captured by solving the partial differential equations (PDEs) on the iced geometry. These are available in ANSYS R19.2 Academic. The basic steps of the solution have been described earlier for a FENSAP-ICE system. Table 1 shows the reference conditions used for the simulation of ice accretion. The reference conditions could be changed depending upon the need of the study.

Table 1: Reference conditions

Characteristic length	0.914 m
Air Velocity	100 m/s
Air Static Temperature	262 K
Air Static Pressure	101325 Pa
Reynolds Number	$7.4136x10^6$
Mach No	0.308
Liquid Water Content	0.0007 kg/m^3
Droplet Diameter	20 microns
Water density	1000 kg/m^3

The airfoil taken for the study is NACA0012. The same has been used in almost all the literatures dealing with ice accretion [27]. The prediction of ice shape, thickness of ice and mass caught during the accretion has been attempted. The extensive validation has been done with the experimental obtained from NASA's icing wind tunnel as reported in Ref.[27].Each module described above runs iteratively in a multi-step process. The selection LWC is based upon the 14 CFR Part 25, Appendix C for continuous maximum icing conditions mentioned in FENSAP-ICE user manual. Some of the key parameters such as free stream icing velocity , duration of icing , airfoil chord length, angle of attack αicing, liquid water content LWC, median volume diameter, ambient temperature and equivalent sand-grain surface roughness define the ice accretion process. Flight velocities are chosen according to typical cruise speeds of aircraft. All CFD calculations are performed by using a steady-state Spalart-Allmaras turbulence model and a streamline upwind artificial viscosity model.

In Fig.1 (a) is shown the contours of velocity magnitude and Fig.1 (b) shows the pressure distribution around the airfoil. The results were produced from the first module: FENSAP which is used for flow calculations. The angle of attack of the flow is zero degree and the stagnation point is at the leading edge (LE) of the airfoil. The maximum pressure observed at LE is 1.033x105 Pa [Reference pressure is 1.01325 x105 Pa] and the maximum velocity magnitude noted during the flow is 6.41 m/s

Fig.1(a) Contours of velocity magnitude

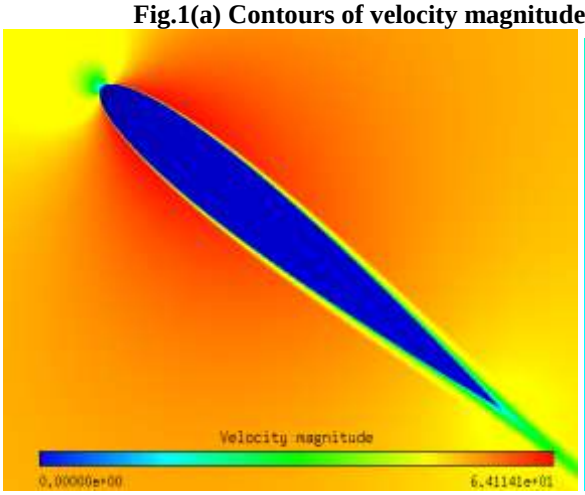

Fig.1(b) Pressure distribution

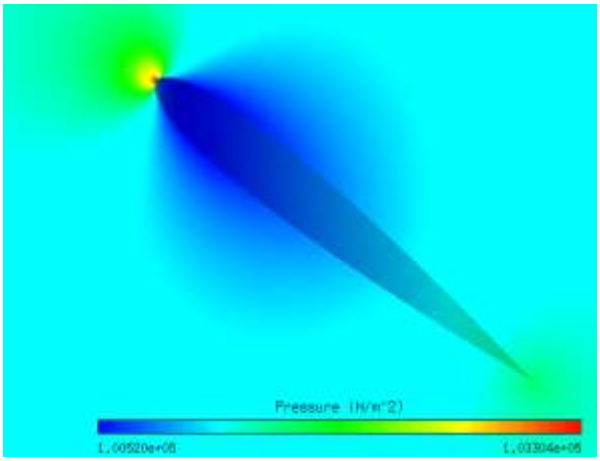

Coordinates used in the study

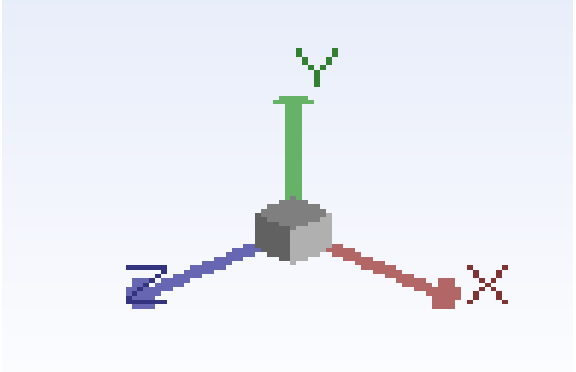

Fig. 2(a) Contours of droplet LWC **Fig. 2(b) Variation of droplet LWC in the LE**

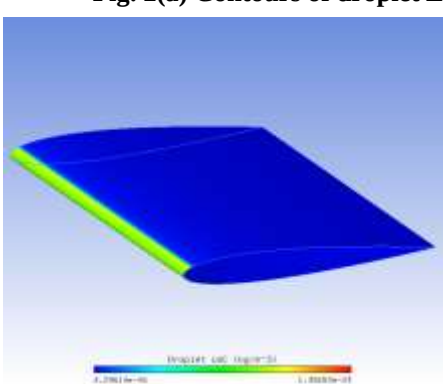

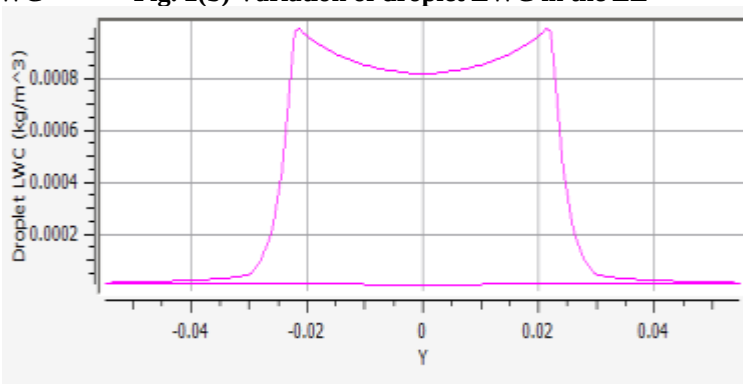

Fig. 3(a) Contours of collection efficiency **Fig. 3(b) Variation of collection efficiency**

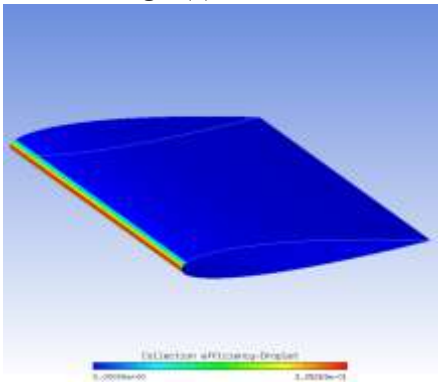

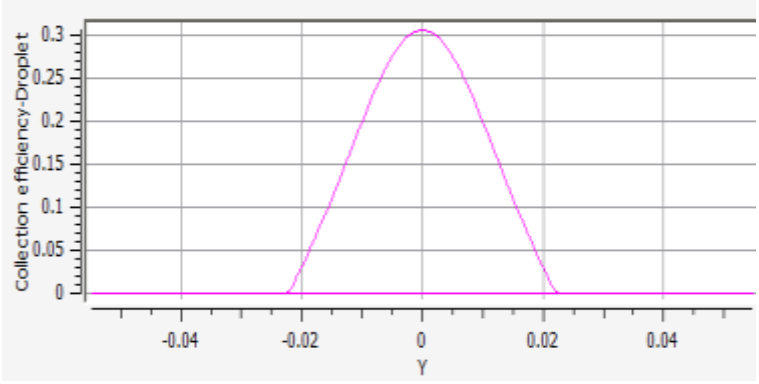

Fig.2(a)-(b) and Fig.3(a)-(b) are showing some of the outputs of the second module: DROP3D. The Fig.2(a) and (b) depict the LWC of droplet at the LE. The more droplet LWC(12.5% rise from the values of LWC at the middle and around 70% up from Y=+/- 0.04) is observed at the upper and lower portions of the LE which is clear in Fig. 2(b). Similarly the highest collection efficiency noted is 0.3 that is shown inFig.3(b) and the same is observed at the middle of LE (Y=0) as shown in Fig.3(a). This is around 30% rise from the collection efficiency at Y=+/- 0.02.

In Fig.4(a) is shown a cut plate across the airfoil where ice accretion has already begun at the reference conditions mentioned above. This is produced from the third module, that is, ICE3D. Fig.4(b) shows the gridding arrangement [chosen from the 3 different grids used for icing simulation] with iced airfoil. The grid independence study has been carried with tolerance values of 10-10 for the convergence of each flow computed variable. The finer grids (1/5th of the size of the largest grid element used) were found near the areas of curvature: Leading Edge(LE) and Trailing Edge(TE) of NACA0012.

Fig.4(a) A cut plane shown across the LE of NACA0012

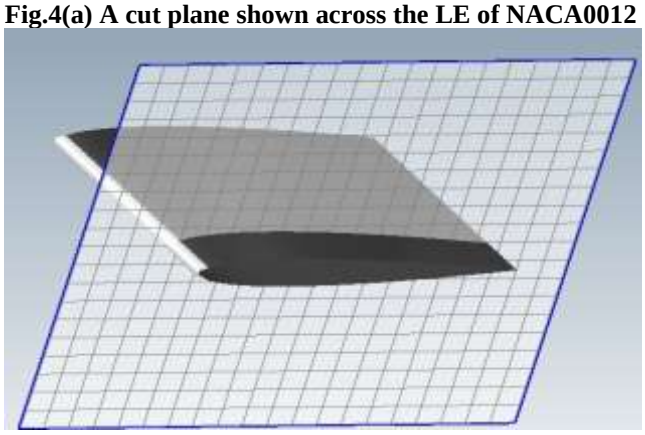

Fig.4(b) Close-up view of grid around the airfoil with ice accreted at LE

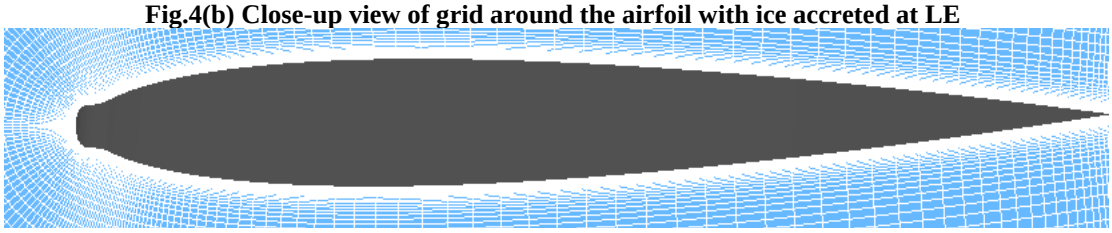

Fig.5(a)-(d) show the comparison of ice thickness with respect to the total time of accretion. The total time of accretion (t_{ice}) was changed in ICE3D solver and the mass of ice caught and thickness of ice over LE were observed. Some typical cases have been presented below. For t_{ice}=5 mins, the total mass of ice was 0.2 kg for t_{ice}=150 mins, the total mass of ice was 5.6 kg . So, it is clear from these plots that the total time of accretion has strong linear correlation with the mass of ice accreted.

Fig 5(a)Time of Accretion = 5 min

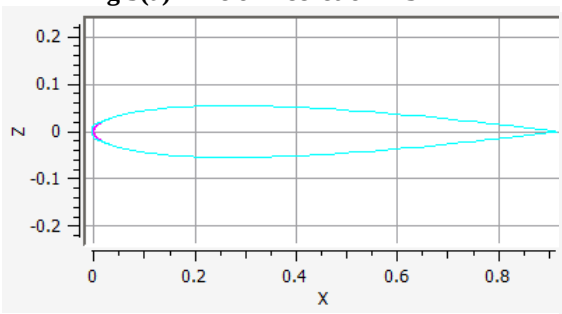

(b) Time of Accretion = 40 min

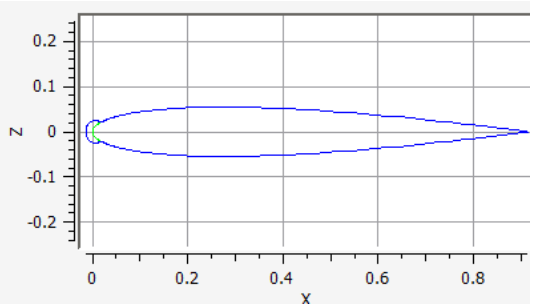

(c) Time of Accretion = 100 min

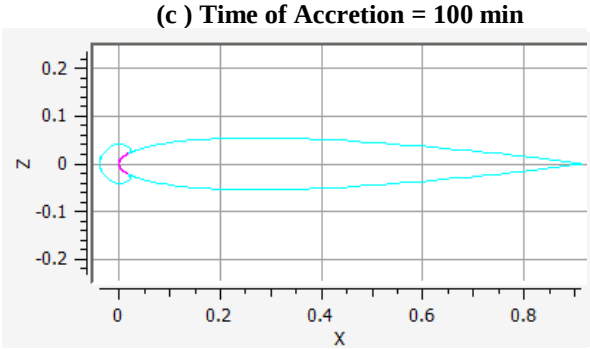

(d) Time of Accretion = 150 min

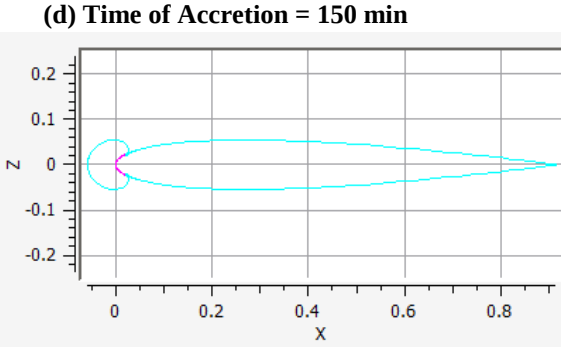

Fig. 6 : Comparison of NACA0012 airfoil before and after ice accretion at Re=7.4x10^6

Before

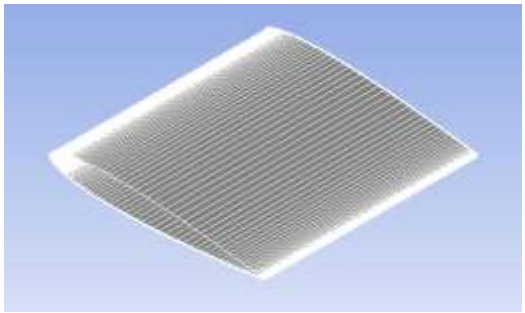

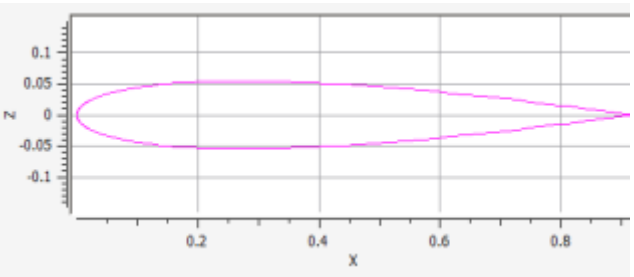

After

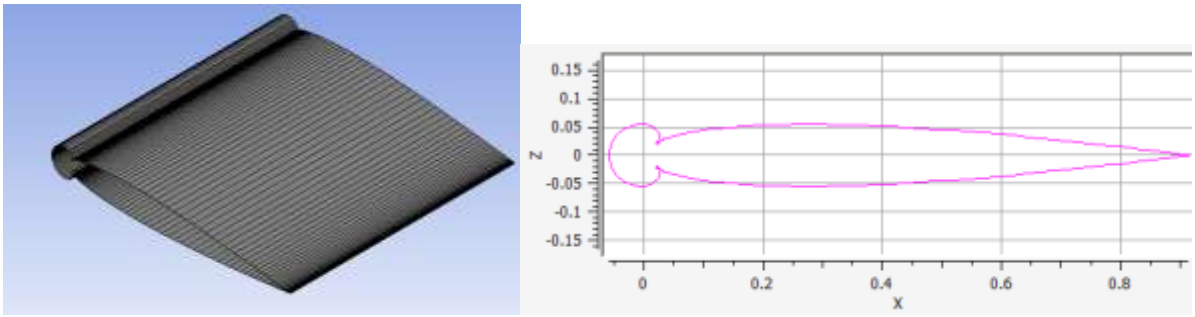

In Fig.6 is shown a typical comparison of NACA0012 airfoil before and after ice accretion phenomenon at Reynolds number (Re)=7.4x10^6.

After understanding the fundamental equations used in the different solvers used in FENSAP-ICE to achieve ice accretion and their interaction with each other through grid file, solution file and configuration settings it was decided to verify and validate the approach and the findings of research. As mentioned earlier that NACA0012 has been taken as a key geometry for the study in the past and for validation purpose, the same was also verified in the present simulation.

In Fig.7(a) is shown a comparison of simulation results of coefficient of lift (CL) for the NACA0012 airfoil for different angles of attack(AOA) with experimental data published in Ref [27]. The matching is fairly well and the same is also observed in Fig.7(b) that shows a comparison of simulation results of coefficient of drag(CD) for the NACA0012 airfoil for different angles of attack(AOA) with experimental data published in Ref [27]. After these two verifications and validation of the approach it was decided to compare and verify the ice accretion in the LE.

In Fig.8 is shown a comparison of simulation of ice accretion for the NACA0012 airfoil with experimental data published in Ref[27]. Though there is a good matching of the trend of ice, obtained from simulation, with the experiment but the amount of ice or thickness does not match.

Fig. 7(a) Comparison of simulation results of coefficient of lift (CL) for the NACA0012 airfoil for different angles of attack (AOA) with experimental data, Ref [27]

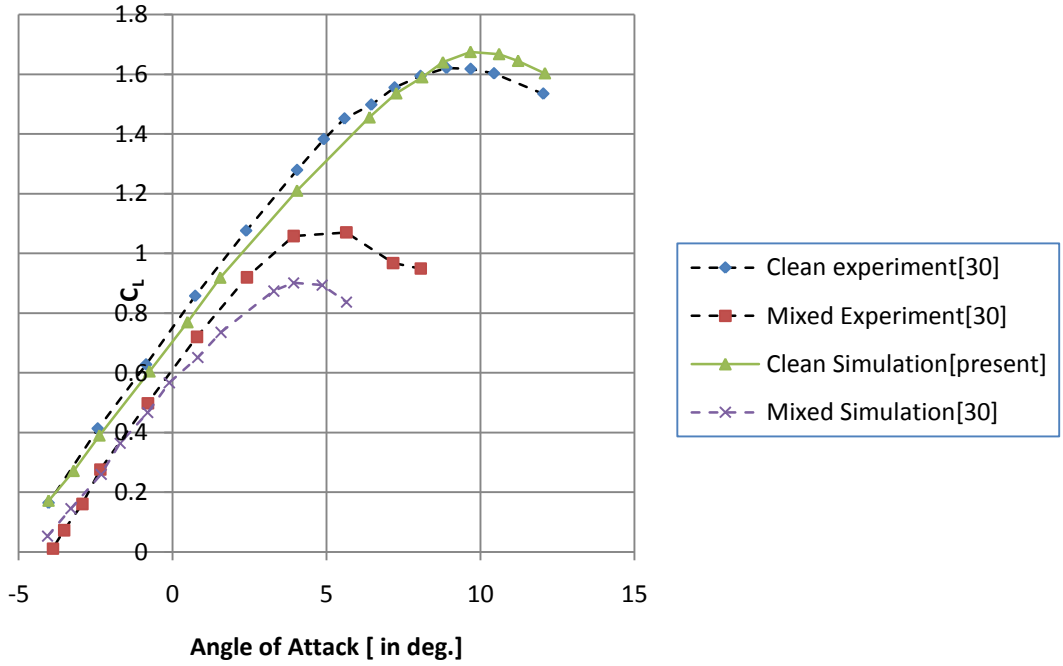

Fig. 7(b) Comparison of simulation results of coefficient of drag(CD) for the NACA0012 airfoil for different angles of attack(AOA) with experimental data, Ref[27]

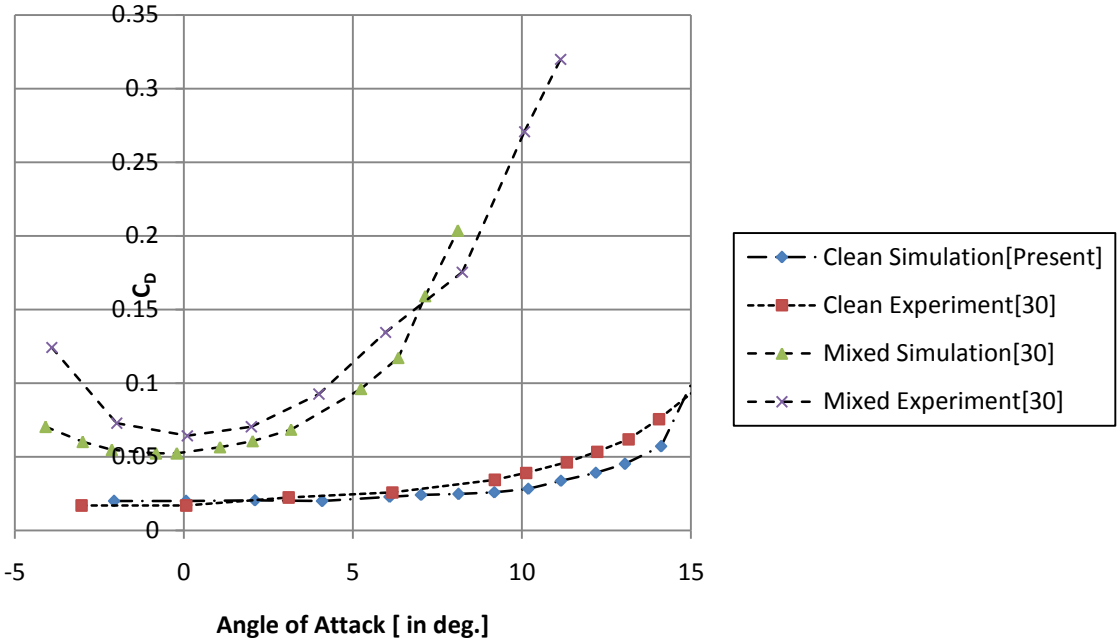

Fig. 8 Comparison of simulation of ice accretion for the NACA0012 airfoil with experimental data, Ref[27]

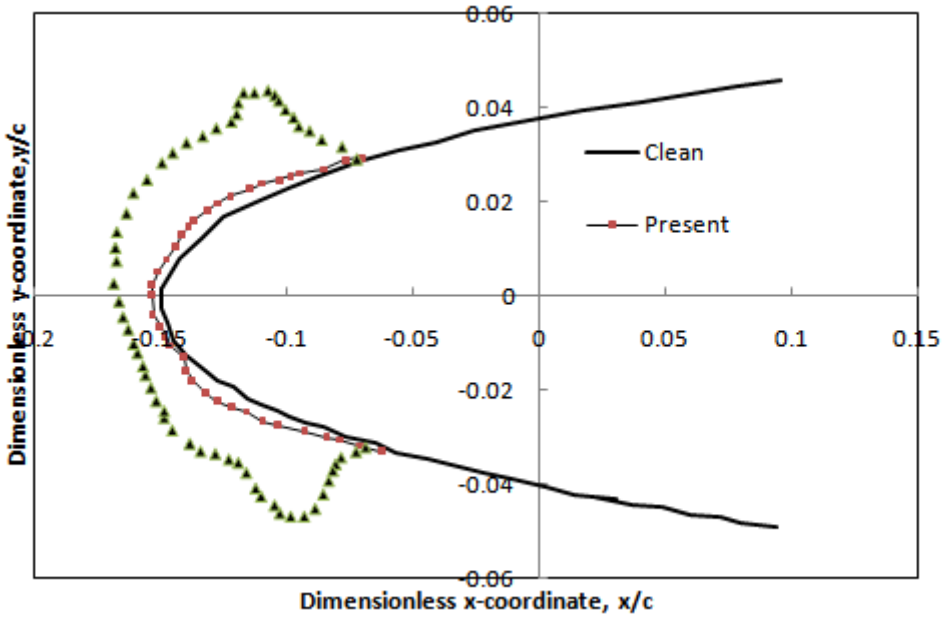

V. CONCLUSION

The ice accretion for NACA0012 airfoil was carried out. The three modules of FENSAP-ICE were used to simulate the ice accretion process over the airfoil surface. The total time of ice accretion has significant impact on the mass of ice formed and ice accreted. The verification and validation of the simulation of ice accretion was done again the experimental data published in Ref [28]. The flow was turbulent for the air flow solution and the accretion was noted during different AOAs . For t_{ice}=5 mins, the total mass of ice was 0.2 kg for t_{ice}=150 mins, the total mass of ice was 5.6 kg. So, it is clear from the investigation the total time of accretion has strong linear correlation with the mass of ice accreted.

ACKNOWLEDGMENT

We thank all the faculties of Aeronautical department, Acharya Institute of Technology for sharing their pearls of wisdom & motivated us during the course of this research.

REFERENCE

[1]. M. Potapczuk, Numerical analysis of a NACA0012 airfoil with leading edge ice accretions, AIAA Paper, No. 0101 (1987).
[2]. A. A. Prikhod′ko, Computer Technologies in Aero hydrodynamics and Heat/Mass Transfer [in Russian], NaukovaDumka, Kiev (2003).
[3]. S. C. Caruso, Development of an unstructured mesh/Navier–Stokes method for aerodynamics of aircraft with ice accretions, AIAA Paper, No. 0758 (1990).
[4]. S. C. Caruso and M. Farshchi, Automatic grid generation for iced airfoil flowfield predictions, AIAA Paper, No. 0415 (1992).
[5]. J. Dompierre, D. J. Cronin, Y. Bourgault, et al., Numerical simulation of performance degradation of ice contaminated airfoils, AIAA Paper, No. 2235 (1997).
[6]. S. Lee and M. B. Bragg, Effects of simulated spanwise ice shapes on airfoils: experimental investigation, AIAA Paper, No. 0092 (1999).
[7]. S. Lee, H. S. Kim, and M. B. Bragg, Investigation of factors that influence iced airfoil aerodynamics, AIAA Paper, No. 0099 (2000).
[8]. H. S. Kim and M. B. Bragg, Effect of leading-edge ice accretion geometry on airfoil aerodynamics, AIAA Paper, No. 3150 (1999). 606
[9]. T. Dunn and E. Loth, Effects of simulated spanwise ice shapes on airfoils: computational investigation, AIAA Paper, No. 0093 (1999).
[10]. S. Kumar and E. Loth, Aerodynamic simulations of airfoils with large-droplet ice shapes, in: Proc. 38th Aerospace Sci. Meeting and Exhibit, Reno NV, AIAA Paper, No. 0238 (2000).
[11]. A. Baumert, S. Bansmer, P. Trontin, P. Villedieu, Experimental and numerical investigations on aircraft icing at mixed phase conditions, International Journal of Heat and Mass Transfer, Volume 123, Pages 957-978 (2018)
[12]. S. V. Alekseenko, Numerical Simulation of the Processes of Hydrodynamics and Heat/Mass Transfer in Regions with Free Boundaries, Candidate′s Dissertation (in Engineering), Dnepropetrovsk (2012).
[13]. A. A. Prikhod′ko and S. V. Alekseenko, Mathematical simulation of the processes of heat and mass transfer in the icing of airfoils, in: Proc. 6th Minsk Int. Heat Mass Transfer Forum "MIF–VI," ITMO im. A. V. Luikova NANB, Vol. 1, Minsk (2008), pp. 1–10.
[14]. A. A. Prikhod′ko and S. V. Alekseenko, Icing of airfoils. Simulation of an air–drop flow, Aviats.-Kosm.Tekh.Tekhnol., No. 4, 59–67 (2013).
[15]. G. Fortin, J. Laforte, and A. Beisswenger, Prediction of ice shapes on NACA 0012 2D airfoil, Anti-Icing Mater. Int. Lab., No. 2154 (2003).
[16]. Fortin G., Ilinca A., and Brandi V. A new roughness computation method and geometric accretion model for airfoil icing. J. Aircraft., 41, No. 1, 119–127 (2004).
[17]. B. L. Messinger, Equilibrium temperature of an unheated icing surface as a function of airspeed, J. Aeronaut. Sci., 20, No. 1, 29–42 (1953).
[18]. F. H. Lozowski, J. R. Stallabras, and P. F. Hearty, The icing of an unheated nonrotating cylinder in liquid water dropletice crystal clouds, National Research Council, Laboratory report No. LTR-LT-96 (1979).
[19]. Ice Accretion Simulation, AGARD-AR-344, Hull (1997).
[20]. W. B. Wright, Users manual for the improved NACA lewis ice accretion code LEWICE 1.6, Contractor Report NACA, May, 1995.
[21]. P. Louchez, G. Fortin, G. Mingione, and V. Brandi, Beads and rivulets modelling in ice accretion on a wing, in: Proc. 36th Aerospace Sci. "Meeting & Exhibit," American Institute of Aeronautics and Astronautics, Reno, Nevada (1998).
[22]. F. H. Ludlam, The heat economy of a rimed cylinder, Q. J. R. Meteor. Soc., 77, No. 1, 663–666 (1951).
[23]. A. P. Broeren, E. A. Whalen, and G. T. Busch, Aerodynamic simulation of runback ice accretion, J. Aircraft, 47, No. 3, 1641–1651 (2010).
[24]. ANSYS® FENSAP-ICE User Manual, Release 18.2,Ansys, Inc.
[25]. Wagdi G. Habashiet. al, Development Of A Second Generation In-Flight Icing Simulation Code, Journal of Fluids Engineering, American Society of Mechanical Engineers, 2006, 128 (2), pp.378-387
[26]. P. Trontin, P. Villedieu. A comprehensive accretion model for glaciated icing conditions. International Journal of Multiphase Flow, Elsevier, 2018, pp.1-10.
[27]. Hann, R., Brandrud, L., Kroegenes, J., Bartl, J., Bracchi, T., and Saetran, L., "Aerodynamic Performance of the NREL S826 Airfoil in Icing Conditions at Low Reynolds Numbers," Unpublished manuscript.
[28]. V. Kashevarov, A & L. Stasenko, A. (2018). Modeling of Ice Accretion on the Airfoil Surface in an Air Flow Containing Ice Particles. Journal of Applied Mechanics and Technical Physics. 59. 645-652.

Swetha S" Numerical Investigation of Ice Accumulation and Accretion over an Airfoil Using FENSAP-ICE Solver" International Journal of Modern Engineering Research (IJMER), vol. 08, no. 11, 2018, pp 29-37